Cleaner Engineering and Technology 13 (2023) 100604

Contents lists available at ScienceDirect

Cleaner Engineering and Technology

journal homepage: www.sciencedirect.com/journal/cleaner-engineering-and-technology

Compressive strength of concrete containing furnace blast slag; optimized machine learning-based models

Mahdi Kioumarsi [a,*], Hamed Dabiri [b], Amirreza Kandiri [c], Visar Farhangi [d]

[a] Department of Built Environment, OsloMet–Oslo Metropolitan University, 0166, Oslo, Norway
[b] Department of Earth Sciences, Sapienza University of Rome & CERI Research Center, P.le Aldo Moro 5, 00185, Roma, Italy
[c] School of Civil Engineering, University College Dublin, Belfield, Dublin 4, Ireland
[d] Department of Civil Engineering, Construction Management, and Environmental Engineering, Northern Arizona University, Flagstaff, AZ, 86011, USA

ARTICLE INFO

Keywords:
Compressive strength
Machine learning
Concrete
GGBFS
Optimization

ABSTRACT

Replacing Ordinary Portland Cement (OPC) with industrial waste like Ground Granulated Blast Furnace Slag (GGBFS) has been proven to have remarkable benefits regarding the mechanical properties of concrete and the environment. The main objectives of this research, as a result, are to (a) develop a generalized, accurate, and optimized Machine Learning (ML)-based model for predicting the compressive strength of concrete incorporating GGBFS and (b) propose equations for easier calculation of the compressive strength of concrete containing GGBFS. To this aim, various ML-based methods, namely Decision Tree (DT), Random Forest (RF), Support Vector Machine (SVM), K-nearest Neighbors (KNN), and Artificial Neural Network (ANN) were considered for predicting the compressive strength of concrete containing GGBFS. An extensive dataset including 625 results of experimental studies was collected from international peer-reviewed publications. The dataset was divided into two sub-datasets: the training dataset (85%), used to train the models on the relationship between input and output parameters, and the testing dataset (15%), used to evaluate the accuracy of the models. The most influential parameters, including ordinary Portland cement, GGBFS grade, GGBFS to cement ratio, water, coarse aggregate, fine aggregate, and testing age, were considered as the input variables for proposing prediction models. The predicted and actual values were compared in each model. The accuracy of the models was also compared using common performance metrics (RMSE, MSE, MAE, MAPE, R, and R^2-score) and Taylor diagram. Eventually, a sensitivity analysis was conducted at the end of the study to explore the influence of GGBFS on cement ratio and GGBFS grade on concrete compressive strength, and consequently, equations were suggested based on the results.

1. Introduction

Concrete is one of the most commonly used construction materials used in different types of structures because of its undeniable advantages (Boğa et al., 2013; Kioumarsi et al., 2020). In recent decades, several studies have been conducted to develop sustainable concrete by partially replacing Ordinary Portland Cement (OPC) with alternative materials (Dabiri et al., 2018; Kandiri et al., 2021). One of the driving motivations for reducing OPC usage in the construction industry is reducing CO_2 emissions associated with its manufacturing (Farahzadi et al., 2022a; Farahzadi et al., 2022b). According to (Benhelal et al., 2013), the manufacturing of OPC accounts for around 7% of worldwide CO_2 emissions. Supplementary Cementitious Materials (SCMs) such as ground granulated blast-furnace slag (GGBS), fly ash (FA) (Chand, 2021; Chand et al., 2021), silica fumes (SF), and rice husk ash (RHA) (Amin et al., 2021) are frequently utilized as partial substitutes for cement in concrete because of their capacity to improve the mechanical and rheological properties of concrete, reduce CO_2 emission, and mitigate adverse environmental consequences. Among various SCMs, Ground Granulated Blast Furnace Slag (GGBFS) is claimed to be an appropriate replacement for cement in terms of ecological, environmental, and mechanical properties of concrete (Bilim et al., 2009; Chidiac and Panesar, 2008). Blast Furnace Slag (BFS) could be defined as a mixture of poorly crystalline phases with composites similar to gehlenite (2CaO.

* Corresponding author.
E-mail addresses: mahdi.kioumarsi@oslomet.no (M. Kioumarsi), hamed.dabiri@uniroma1.it (H. Dabiri), amirreza.kandiri@ucdconnect.ie (A. Kandiri), visar.farhangi@nau.edu (V. Farhangi).

https://doi.org/10.1016/j.clet.2023.100604
Received 23 September 2022; Received in revised form 7 February 2023; Accepted 11 February 2023
Available online 13 February 2023

$Al_2O_3.SiO_2$) and akermanite ($2Cao.MgO.2SiO_2$), as well as depolymerized calcium silicate glasses (Duxson, 2009). BFS is a by-product of blast furnaces' iron production, which is a mixture of iron-ore, coke, and limestone (Cwirzen, 2020; Amin et al., 2017). BFS is rapidly cooled by powerful water jets or in a water pound to be formed into a fine, granular, almost entirely non-crystalline, glassy form known as granulated slag, which exhibits appropriate cementitious properties when finely ground and combined with Portland cement (Oner and Akyuz, 2007; Wang et al., 2020).

1.1. Brief literature review on the application of GGBFS in concrete

Several studies proved that the application of GGFBS as a supplementary cementitious material in concrete has many advantages: (1) improving the long-term strength of concrete, (2) improving durability, (3) reducing porosity, (4) improving the interface with aggregate, (4) energy and environmental benefits due to reduction in cement supplying and therefore, decreasing CO_2 emission, (5) better engineering and performance properties of concrete because of using mineral admixtures with appropriate size distribution characteristics and pozzolanic and cementitious reactivity (Chidiac and Panesar, 2008; Lee et al., 2006), (6) reducing concrete permeability and preventing reinforcement corrosion (Boğa et al., 2013), and eventually (7) being more economical in terms of construction cost since cement is replaced by GGBFS (Wang et al., 2020). The only shortcoming of using GGBFS is lower resistance to deicer salt scaling when tested at 25 days. This might be because of slow hydration and insufficient curing regime for concrete containing GGBFS (Chidiac and Panesar, 2008). Since this study aims to compare different machine learning-based methods for predicting the compressive strength of concrete with GGBFS, the deeper details of the effect of utilizing GGBFS on concrete performance are not discussed for the sake of shortness, and the interested readers are referred to the above-mentioned references and similar studies (Cheng et al., 2005; Bhojaraju et al., 2021).

1.2. ML-based methods proposed for GGBFS concrete

Over the past decades, considerable studies have developed around the application of artificial intelligence (AI) and machine learning (ML) methods in different fields of science as well as civil engineering. Among various aspects of engineering which might be considered for the application of ML (e.g., structural health monitoring, failure modes, the behavior of elements, etc.), predicting mechanical properties of materials employing ML approaches is more popular than other issues (Moradi et al., 2020; Bypour et al., 2021). It could be due to its benefits, such as (i) high accuracy in predicting models and (ii) being quick, simple and inexpensive in comparison to complicated, time-consuming and costly experimental studies (Ahmadi et al., 2020; Dabiri et al., 2022a).

To the best of the authors' knowledge, a limited number of studies have been conducted to develop an ML-based model for predicting the mechanical properties of concrete containing GGBFS. Table 1 provides a literature review on the application of ML-based methods for determining the properties of GGBFS concrete. The studies mentioned in Table 1 utilized different databases for developing ANN and ML-based models, and consequently, the characteristics of the models are not the same.

2. Research significance and objective

In this study, an attempt has been made to predict the compressive strength of concrete containing GGBFS using different ML-based approaches, namely Decision Tree (DT), Random Forest (RF), Support Vector Machine (SVM), K-nearest Neighbors (KNN), and Artificial Neural Network (ANN). The gap in the previous studies and the significance of the current study could be listed as below:

(a) The most notable significance of the present research is the sensitivity analysis performed for better understanding the effect of GGBFS to cement ratio and GGBFS grade on concrete compressive strength. In addition, the results of the parametric study were implemented to obtain equations that could be used for calculating the compressive strength of concrete containing GGBFS with different grades at different testing ages.
(b) As can also be figured out from Table 1, the previous studies have focused on the ANN technique. Other ML-based methods have been either less concerned (e.g., SVM) or not used so far (e.g., DT, KNN) for developing prediction models determining the compressive strength of GGBFS concrete. As a result, in addition to ANN and RF, other methods, including SVM, DT, and KNN, are considered for predicting the compressive strength of concrete incorporating GGBFS for the first time in this study.
(c) Most of the previously proposed prediction models are based on databases with limited samples. This might affect the models'

Table 1
A review on the application of ML-based methods for predicting properties of concrete incorporating GGBFS.

Reference	Aim of study	Number of samples	ML-based models	Investigated parameters
Boga et al. (Boğa et al., 2013)	Analyzing properties of concrete incorporating GGBFS and calcium nitrite-based corrosion inhibitor (CNI)	162	ANN and ANFIS	compressive strength, splitting tensile strength, chloride ion permeability, durability
Shahmansouri et al. (Shahmansouri et al., 2020)	Predicting the compressive strength of geopolymer concrete based on GGBS	351	Gene Expression Programming (GEP)	compressive strength
Saridemir et al. (Sarıdemir et al., 2009)	Predicting long-term effects of GGBFS on compressive strength of concrete under wet curing conditions	284	ANN and Fuzzy Logic	compressive strength
Bilim et al. (Bilim et al., 2009)	Predicting the compressive strength of GGBFS concrete	225	ANN	compressive strength
Kandiri et al. (Kandiri et al., 2020)	Estimating the compressive strength of concretes containing GGBFS	624	ANN with Multi-Objective Slap Swarm Algorithm (MOSSA), M5P	compressive strength
Mohana (Mohana, 2020)	Predicting compressive strength of GGBFS concrete	268	Random Forest and SVM	compressive strength
Mai et al. (Mai et al., 2021a)	Predict compressive strength of concrete containing BFS and fly ash (FA)	1274	ANN	compressive strength
Mai et al. (Mai et al., 2021b)	Determining compressive strength of concrete containing GGBFS	453	Random Forest	compressive strength
Ozcan et al. (Ozcan et al., 2017)	Assessing the effect of BFS and waste tire rubber powder (WTRP) on the compressive strength of cement mortars	288	Random Forest, Ada Boost, SVM and Naïve Bayes Classifier	compressive strength

accuracy and reliability when implemented for a new dataset (Boğa et al., 2013; Mai et al., 2021a). The present study uses an extensive database, including 625 samples, for training and testing the proposed models. Furthermore, the concrete compressive strength of the samples considered in the present study is in the range of 3.40–80.32 MPa. Therefore, the proposed models, which cover this broad range of compressive strength, could be ideally used for numerous concrete mixtures investigated by researchers in future studies.

(d) The accuracy of an ML-based prediction model undoubtedly has a pivotal role in its reliability. As a result, a comparative study on the performance of different ML-based methods is needed. In this study, the methods mentioned above are compared and discussed extensively.

(e) More importantly, a high-accurate prediction model could help researchers evaluate the effects of GGBFS on the compressive strength of concrete in simpler, quicker, and more economical method than time-consuming and pricy experimental studies.

This research analyzes the compressive strength of concrete containing GGBFS using various machine learning-based models. The goal is to optimize the prediction of compressive strength by comparing the results of different models using standard performance metrics and Taylor diagrams. The study utilizes a comprehensive database to train and evaluate the models. The most accurate model will be identified, and its equation will be presented for practical use in determining the compressive strength of concrete with GGBFS. The study flowchart is depicted in Fig. 1, clearly visualizing the research process. Overall, this research offers a comprehensive analysis of the compressive strength of concrete incorporating GGBFS, utilizing cutting-edge machine learning techniques to provide accurate predictions.

3. Database collection

Totally 625 test results are gathered from 625 experimental tests conducted on the compressive strength of concrete containing GGBFS (Boğa et al., 2013; Bilim et al., 2009; Chidiac and Panesar, 2008; Oner and Akyuz, 2007; Lee et al., 2006; Li and Zhao, 2003; Sengul and Tasdemir, 2009; Becknell and Hale, 2005; Arivalagan, 2014; Deboucha et al., 2015; LaBarca et al., 2007; Cramer and Sippel, 2005; Samad et al., 2017; Anand et al., 2017; El-Hassan and Kianmehr, 2018; Gowri et al., 2016; Sridevi et al., 2016; Dabhekar et al., 2017; Nagendra et al., 2016; Kumar et al., 2017; abhekar et al., 2017). It is worth explaining that the concrete compressive strength (CCS) in the collected database is the test results on either cylindrical or cubic samples. This research considers the cylinder (150 × 300 mm) compressive strength. The cubic compressive strength is converted to the equivalent cylindrical strength ($CCS_{cylindrical} = 0.80 \times CCS_{cubic}$). The variable parameters considered in all the research studies, as mentioned above, are ordinary Portland cement (OPC, kg/m^3), GGBFS to cement ratio (G/C), GGBFS grade, water (W, kg/m^3), coarse aggregate (CA, kg/m^3), fine aggregate (FA, kg/m^3), testing age (days). Since test parameters have a notable effect on the concrete compressive strength (CCS, MPa), they are all considered as inputs for the prediction models as well, and the only output is concrete compressive strength. Table 2 provides the statistical properties of the inputs and output.

According to the data in Table 2, the concrete compressive strength of all the samples is 3.40–80.32 MPa, which covers quite an extensive range. It simply means that the proposed models could be used for concrete mixtures with compressive strength in the aforementioned range. The distribution of the output and input parameters is also illustrated graphically in Fig. 2. It should be explained that the vertical axe in the diagrams represents the number of collected data corresponding to each parameter's value. In contrast, the horizontal axe refers to each parameter's value considered in this study. Otherwise mentioned, Fig. 2 depicts the amount of data collected for each value of the considered input and output variables. As an example, the last diagram demonstrates that a considerable portion of the collected concrete samples has a compressive strength in the range of 20–40 MPa.

Considering the variables with a high effect on the target output is critical for developing an accurate model. In order to figure out which parameters have the highest and lowest effect on the output, the correlation between parameters should be determined. Among various correlations introduced so far (e.g., Intra-class, Rank), the Pearson method is more common among researchers (Nettleton, 2014; Williams et al., 2020). Pearson correlation coefficient (PCC) is defined as the ratio of covariance of two parameters, *cov* (X, Y), to the multiplication of their standard deviation, $\sigma_x\sigma_y$, as given in Eq. (1):

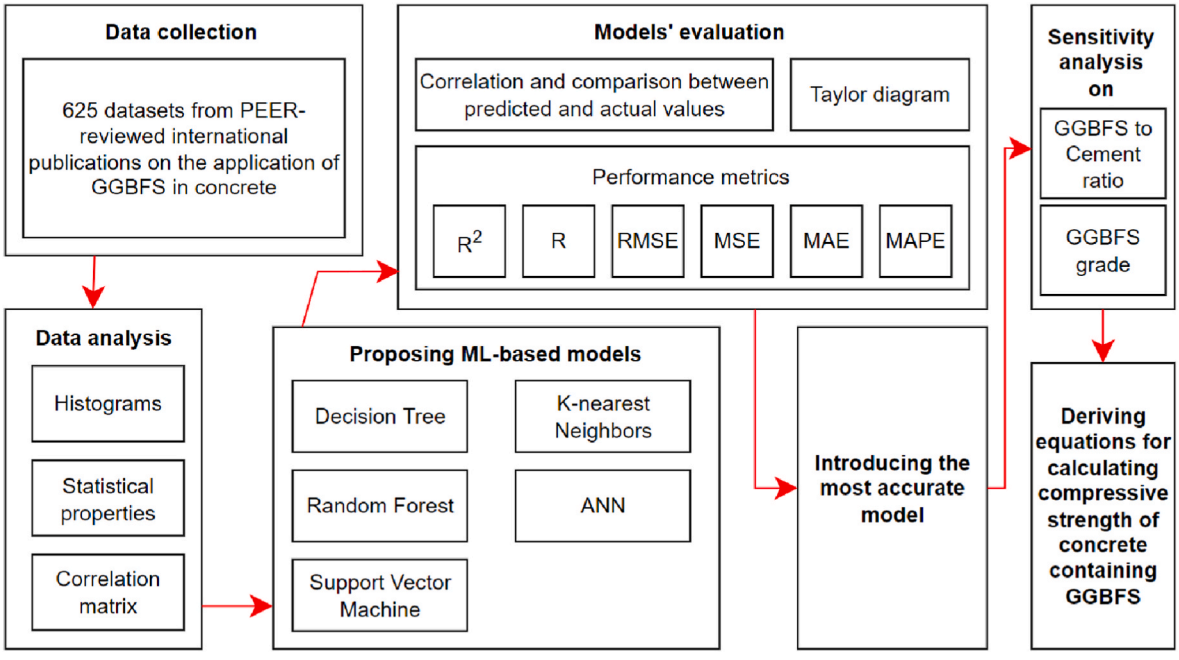

Fig. 1. Research flowchart.

Table 2
Statistical properties of the input and output parameters.

	Minimum	Maximum	Mean	Median	Variance	STD
OPC (kg/m^3)	70.00	450.00	241.81	235.50	4863.17	69.74
GGBFS/Cement	0.00	4.00	0.62	0.42	0.51	0.72
GGBFS grade	80.00	120.00	101.03	100.00	163.31	12.78
W (kg/m^3)	83.70	295.00	186.07	150.70	2032.40	45.08
CA (kg/m^3)	723.00	1166.00	1037.71	1102.30	10651.59	103.21
FA (kg/m^3)	477.00	1328.00	743.77	733.90	23564.12	153.51
Age (days)	1.00	365.00	86.46	28.00	14998.94	122.47
CCS (MPa)	3.40	80.32	29.15	27.96	136.32	11.68

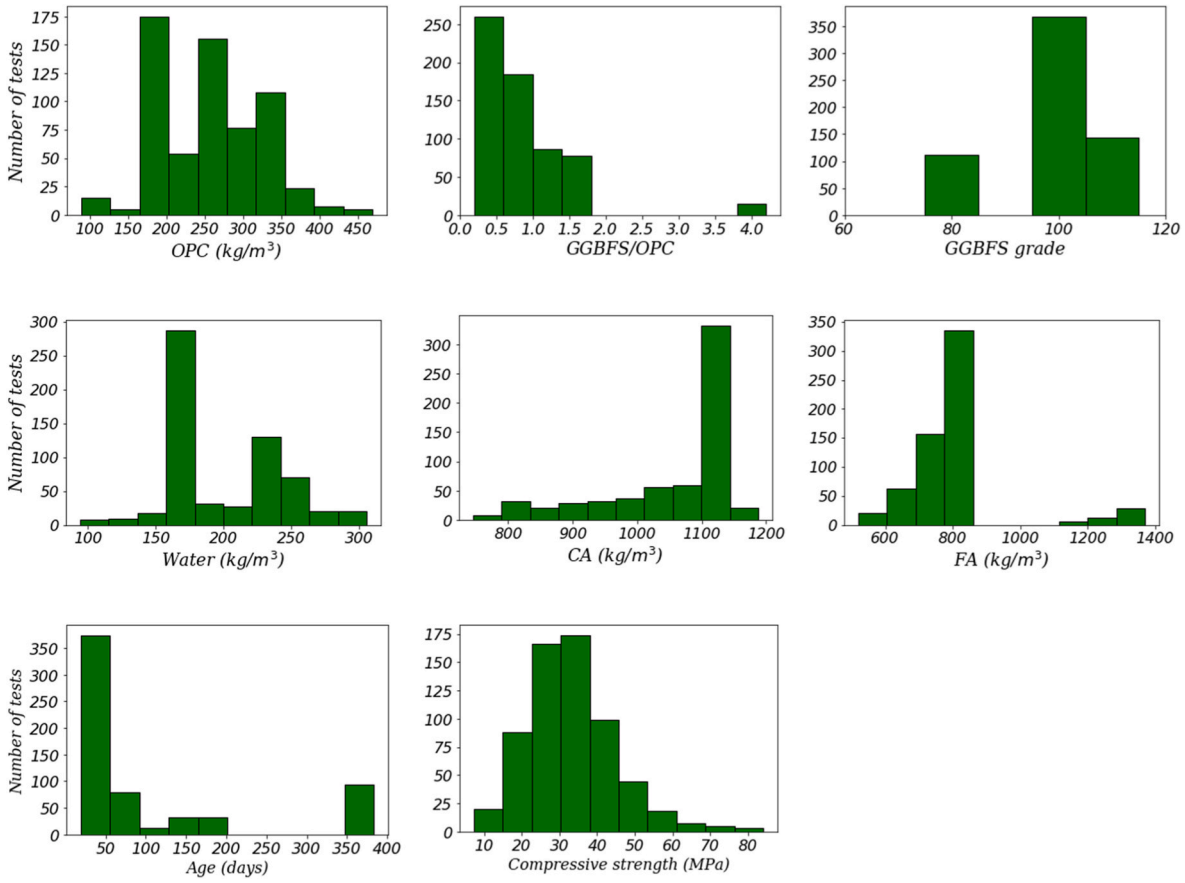

Fig. 2. Graphical illustration of the output and input parameters.

$$\rho_{X,Y}=\frac{\mathrm{cov}(X,Y)}{\sigma_X\sigma_Y}=\frac{\sum(x_i-\overline{x})(y_i-\overline{y})}{\sqrt{\sum(x_i-\overline{x})^2}\sqrt{\sum(y_i-\overline{y})^2}} \quad (1)$$

where $\overline{x}$ and $\overline{y}$ are the mean of X and Y datasets, respectively and $\rho_{X,Y}$ is Pearson correlation coefficient which is in the range of (−1,1); $\rho_{X,Y}=1$ stands for their high correlation while $\rho_{X,Y}=0$ reflects the linear independence of X and Y. It should be explained that since Pearson correlation shows a linear relationship, $\rho_{X,Y}=0$ does not mean that the parameters do not correlate. Still, they might have a nonlinear correlation (Kotu and Deshpande, 2018). It is worth stating that a negative correlation means an inverse relationship between two parameters (Berman, 2016). Table 3 presents the Pearson correlation coefficient matrix of the inputs and output. According to Table 3, coarse aggregate,

Table 3
Pearson correlation coefficients of the parameters considered in the models.

	OPC (kg/m^3)	G/C	GGBFS grade	W (kg/m^3)	CA (kg/m^3)	FA (kg/m^3)	Age (days)	CCS (MPa)
OPC (kg/m^3)	1							
G/C	−0.5546	1						
GGBFS grade	0.0503	−0.2955	1					
W (kg/m^3)	0.0002	0.2793	−0.2039	1				
CA (kg/m^3)	−0.0888	−0.3877	0.525	−0.4268	1			
FA (kg/m^3)	0.0279	−0.1745	−0.3518	−0.6036	−0.2302	1		
Age (days)	−0.0242	0.0031	0.0312	0.1669	0.0432	−0.1916	1	
CCS (MPa)	**0.2344**	**−0.0179**	**−0.1773**	**−0.0213**	**−0.4345**	**0.2275**	**0.3772**	**1**

testing age, and OPC have the highest correlation with the compressive strength of concrete since they have a key effect on the concrete strength. On the other hand, G/C exhibits the lowest correlation among other input variables.

4. Models

In this section, the ML-based methods are defined, and then the characteristics of the proposed prediction models are explained.

4.1. Decision Tree (DT)

The Decision Tree method is a supervised ML technique that could be applied to classifications and regression problems. When the target output is a continuous value, regression DT is used, while classification DT is utilized for non-continuous values. This method is called Decision Tree because it uses a tree-shape graph for predicting the target output: the leaf nodes correspond to the class label and the branches are the features (or conditions) of the class labels (Liu et al., 2015; Bellini, 2019). DT approach has many advantages, including (a) being simple to understand, interpret and visualize, (b) capable of being used for both classification and regression problems, (c) having the possibility of incorporating decision technique with a decision tree, and (d) having the asset of modeling a high degree of nonlinearity in the relationship between the target output and the input variables (Nisbet et al., 2009; Shobha and Rangaswamy, 2018). On the other hand, being prone to overfitting and having difficulty in classifying multiple output classes are reported as shortcomings of this approach (Nisbet et al., 2009).

4.2. Random Forest (RF)

One of the elaborations of DT is the Random Forest approach which Breiman introduced in 2001 by combining classification and regression trees and bagging (Fawagreh et al., 2014; Breiman, 2001). RF contains many decision trees, which trains several trees in parallel by bootstrapping technique and considers the average of the predictions made by trees as the target output. Overall, RF is an ensemble classifier based on bootstrap, followed by aggregation (Dabiri et al., 2022b). The benefits of RF are: (a) high accurate results in the case of using large databases, (b) being simple and fast to implement, and (c) higher accuracy in comparison to other ML-based methods, as reported in many research studies (Nisbet et al., 2009).

As could be figured out from the above-mentioned explanations, the number of trees is a critical factor in the accuracy of an RF model. Fig. 3 demonstrates the number of trees against the R^2-score for finding the number of trees, which leads to the highest accuracy. As observed, the highest R^2 (0.97) belongs to the model with 66 trees; therefore, this model is considered for predicting the compressive strength of concrete with GGBFS.

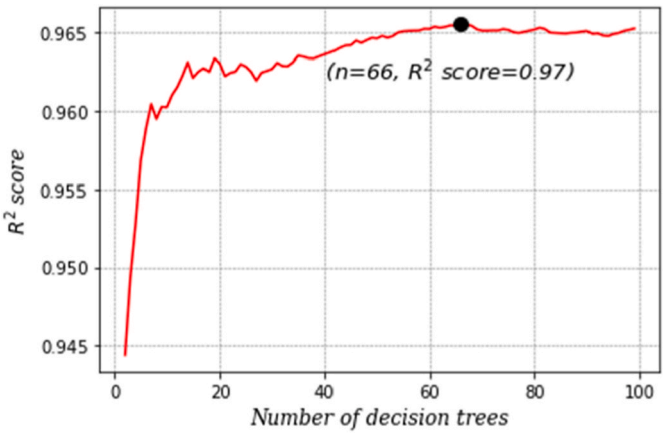

Fig. 3. R^2-score values were obtained for the different numbers of trees in the proposed RF model.

4.3. Support Vector Machine (SVM)

Support Vector Machine, developed by Vapnik (Cortes and Vapnik, 1995; Vapnik, 1999), is a supervised training algorithm based on statistical learning theory (Satapathy et al., 2019). The method creates hyperplanes to classify the features. From the viewpoint of mathematics, SVM could be expressed as:

Minimizing $\frac{1}{2}\|w\|^2 + C\sum_{i=1}^{N}(\xi_i + \xi_i^*)$ *Subjected to the linear loss function defined in the limits as below:*

$$\begin{cases} y_i - w\varphi(x_i) - b - \xi_i \le \varepsilon & (2.a) \\ -y_i + w\varphi(x_i) + b - \xi_i^* \le \varepsilon & (2.b) \\ \xi_i, \xi_i^* \ge 0 & (2.c) \end{cases}$$

where y_i represents the estimated values, $\varphi(x)$ is a nonlinear mapping function, w stands for the matrix showing the position of the hyper-plane for N data points and ξ_i and ξ_i^* is the difference between the actual values and uncertainty margins (see Fig. 4) (Mishra, 2021). The best plate is the one maximizing the margin between the two classes. Consequently, the support vectors are the closest data points to the hyperplane (Dukart, 2015). The explanations, as mentioned earlier, are displayed schematically in Fig. 4.

4.4. K-nearest Neighbors (KNN)

Fix and Hodges (1989) introduced the K-nearest Neighbors algorithm and Joseph Hodges in 1951 and then was modified by Cover and Hart (1967). KNN is a supervised ML-based algorithm that can be used for classification and regression problems (Mishra, 2021). KNN is based on finding K closest samples in the attribute space (Shokrzade et al., 2021). The distance and similarity functions are the main factors that considerably affect the predicted value's accuracy (Bhattacharya et al., 2017). The most known function for continuous variables used in KNN regression is Minkowski (Eq. (3)). It is worth noting that by considering $p = 1$ and $p = 2$, the Minkowski distance function will be known as Manhattan and Euclidean distance functions, respectively.

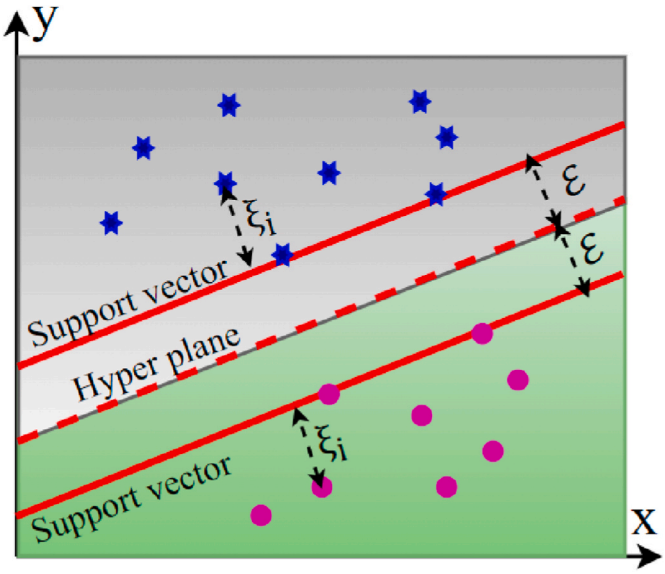

Fig. 4. Schematically illustration of SVM.

$$\left(\sum_{i=1}^{N}|(X_i - Y_i)|^p\right)^{1/p} \quad (3)$$

where X_i and Y_i are two data points in an N-dimension space (in our model, $N = 2$). A simple application of KNN is to introduce the average of the K-nearest samples to the actual sample as the predicted target output. Therefore, the optimum number of K neighbors could significantly lead to the most accurate results (Naik et al., 2021).

The KNN model proposed in this study uses the Euclidean distance function (p = 2). Furthermore, according to the process of finding the most optimum K shown in Fig. 5, seven neighbors resulted in the highest accuracy ($R^2 = 0.85$).

4.5. Artificial Neural Network (ANN)

The Artificial Neural Network is a nonlinear model similar to the complicated biological nervous system function of the human brain (Abiodun et al., 2018; Chaabene et al., 2020). This popular and accurate method has been increasingly applied in various fields, including social science, art, and engineering (Abiodun et al., 2018). The main components of an ANN model are artificial neurons, connections, weights, and activation functions. The information propagation is performed through the connections that get the neurons' data to deliver to the next neurons (Abiodun et al., 2018; Chaabene et al., 2020). Each connection is assigned a weight that reflects the significance of its input on the output. Each neuron combines the information received from other neurons with an activation function and then sends it to the following neuron. This iteration process is continued until an acceptable predicted output is reached (Golafshani et al., 2012). In general, an ANN model is formed by an input layer, hidden layer(s), and an output layer. The number of neurons in the input layer is the same as the number of variables considered inputs. The number of hidden layers, on the other hand, might vary for each model and affect the accuracy of the results noticeably. The activation function could be considered for hidden and output layers, while a bias value could be considered for input and hidden layers. In the framework of mathematics, the output could be formulated as Eq. (4) (Mishra, 2021):

$$O_j = f\sum\left(w_{ij}I_i + b\right) \quad (4)$$

where O_j is the predicted target output, wij is the weight, Ii is the input variable, and b is bias.

The optimized architecture of an ANN model could be developed by trial and error (Mishra, 2021). The final ANN model obtained for predicting the compressive strength of concrete incorporating GGBFS, contains ten inputs, two hidden layers with nineteen neurons in each layer. The Scaled Exponential Linear Units (SELU) activation function (Eq. (5)) (Klambauer et al., 2017) and 20 batch sizes were considered for the model. Bias value was also considered for all the hidden and input layers. Fig. 6 compares the number of neurons with the corresponding R^2-score for the proposed model. The architecture of the final proposed ANN model is displayed in Fig. 7.

$$f(x) = Selu(x) = \lambda\begin{cases} x & x \geq 0 \\ \alpha(e^x - 1) & x < 0 \end{cases} \quad (5)$$

$$\alpha \approx 1.6733 \quad \lambda \approx 1.0507$$

5. Results

In this section, the predicted values obtained by each model are graphically compared with the actual values of both sub-databases (training and testing). Fig. 8 shows the correlation between the predicted and actual values, while Fig. 9 compares the predicted values with the corresponding actual value.

The comparison made in Figs. 8 and 9 confirms the high ability of the proposed models to learn the relationship between the input parameters and the output. Based on the graphical comparison illustrated in Figs. 8 and 9, it could be stated that the model DT possesses the highest accuracy while the model KNN shows the lowest accuracy. All the models, however, exhibited acceptable reliability. The quantitative comparison between the models is presented in the following section to reach a more proper conclusion.

6. Accuracy evaluation

The prediction models could be evaluated through different approaches. The present study assesses the models by (a) common performance metrics and (b) Taylor diagram.

6.1. Performance metrics

The most common performance metrics which reflect the accuracy of a prediction model are R^2, R, root mean square error (RMSE), mean square error (MSE), mean absolute error (MAE), and mean absolute percentage error (MAPE). The fundament of the above-mentioned parameters is based on the difference between the actual and the corresponding predicted value. The obtained performance metrics for all the models are reported in Table 4.

As can be observed in Table 4, the DT and RF models are the most accurate models with the highest R^2 (0.94). Conversely, the model KNN possesses the lowest accuracy. It could also be claimed that all the models with an R^2-score higher than 0.85 exhibited high reliability for predicting the compressive strength of concrete containing GGBFS.

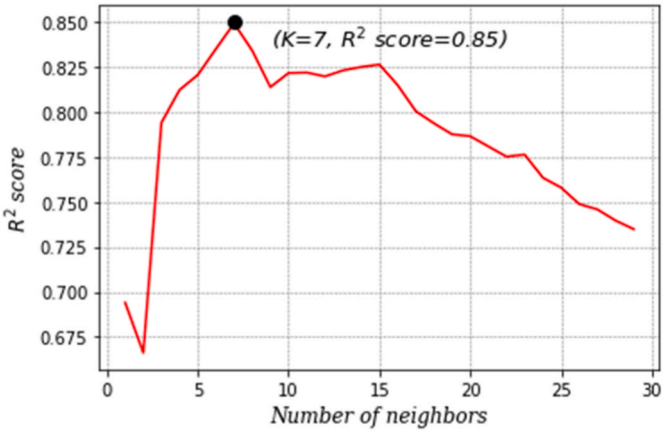

Fig. 5. Finding the optimum number of neighbors in KNN.

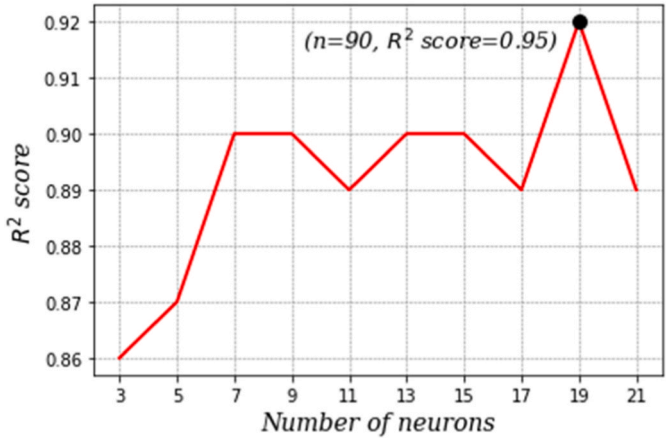

Fig. 6. R^2-score versus the number of neurons in hidden layers for the ANN model.

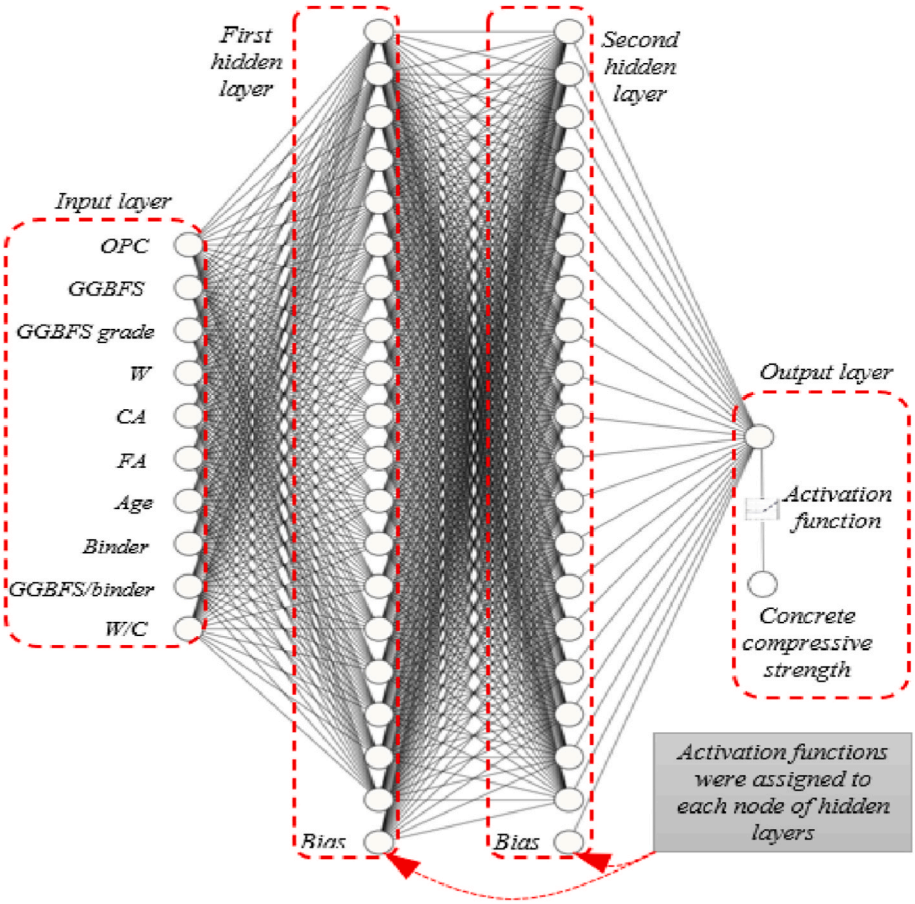

Fig. 7. The architecture of the final ANN model.

6.2. Taylor diagram

Taylor diagram is one of the most useful approaches for evaluating the performance of prediction models. This diagram illustrates the most reliable and, thus, the most accurate model by comparing its distance to the reference point (actual values) (Band et al., 2021; Taylor, 2001). The position of a model is determined by three parameters: standard deviation (vertical and horizontal axis), correlation coefficient (radial lines) and RSME (circular lines centered at the actual value point). The closest model to the reference point is considered the most accurate model (Band et al., 2021).

The proposed prediction models are compared in the Taylor diagram shown in Fig. 10. The DT and RF models are the closest points, while the KNN model is the farthest to the reference point (blue star). Therefore, as reported previously in Table 4, the DT and RF models with the highest R^2, lowest RMSE, and standard deviation are introduced as the most accurate ML-based methods for predicting the compressive strength of concrete incorporating GGBFS.

7. Sensitivity analysis

The sensitivity analysis aims at realizing the effect of GGBFS grade and value on the compressive strength of the concrete mixture. To this end, a test result is considered from an experimental study available in the literature (Bilim et al., 2009). Then, a database including 23 data was generated by altering the ratio of GGBFS to cement in the range of 0–1 with the step of 0.2 for 3-day, 7-day and 28-day testing age (six datasets for each testing age as given in Table 5, rows 1–6, 7–12 and 13–18, respectively). The compressive strength of the generated database was predicted by the RF model, which showed a high-performance accuracy.

The effect of GGBFS grade was also assessed by generating three datasets with different GGBFS grades (80–120 by the step of 20) and predicting their compressive strength using the previously developed RF model (rows 19–23 of Table 5). It is worth noting that other materials of the generated concrete mixtures were considered unchanged. Table 5 presents the predicted values and their difference with the reference mixture. The variation of f'_c due to G/C value and grade is graphically depicted in Fig. 11 and Fig. 12, respectively. It should be explained that for an easier understanding of the influence of G/C value and grade on concrete compressive strength, the vertical axe of Figs. 11 and 12 are normalized by being divided to f'_c of normal concrete without GGBFS, and f'_c of concrete containing GGBFS grade 80, respectively. This normalization could result in more generalized equations provided later in this section.

Taking Table 5 and Fig. 11 into account, it could be figured out that by increasing GGBFS, generally, concrete compressive strength decreases. However, the reduction rate is not constant. In other words, by replacing cement with GGBFS up to almost 40%, f'_c decreases slightly (up to 16.38%). For GGBFS to cement ratio = 0.60, f'_c reduces considerably (up to 43.12%), and eventually, it remains roughly unchanged for GGBFS to cement ratio higher than 0.80. Overall, it could be claimed that replacing cement with GGBFS, up to 40%, does not affect the compressive strength of concrete considerably and thus could be recommended regarding its benefits in terms of environment and construction cost. The f'_c variations observed in this section due to adding GGBFS in concrete align with the results of similar experimental studies (Boğa et al., 2013; Sengul and Tasdemir, 2009). Moreover, based on the parametric study results, prediction equations with high accuracy values ($R^2 \geq 0.86$) are obtained and suggested for calculating f'_c of concrete

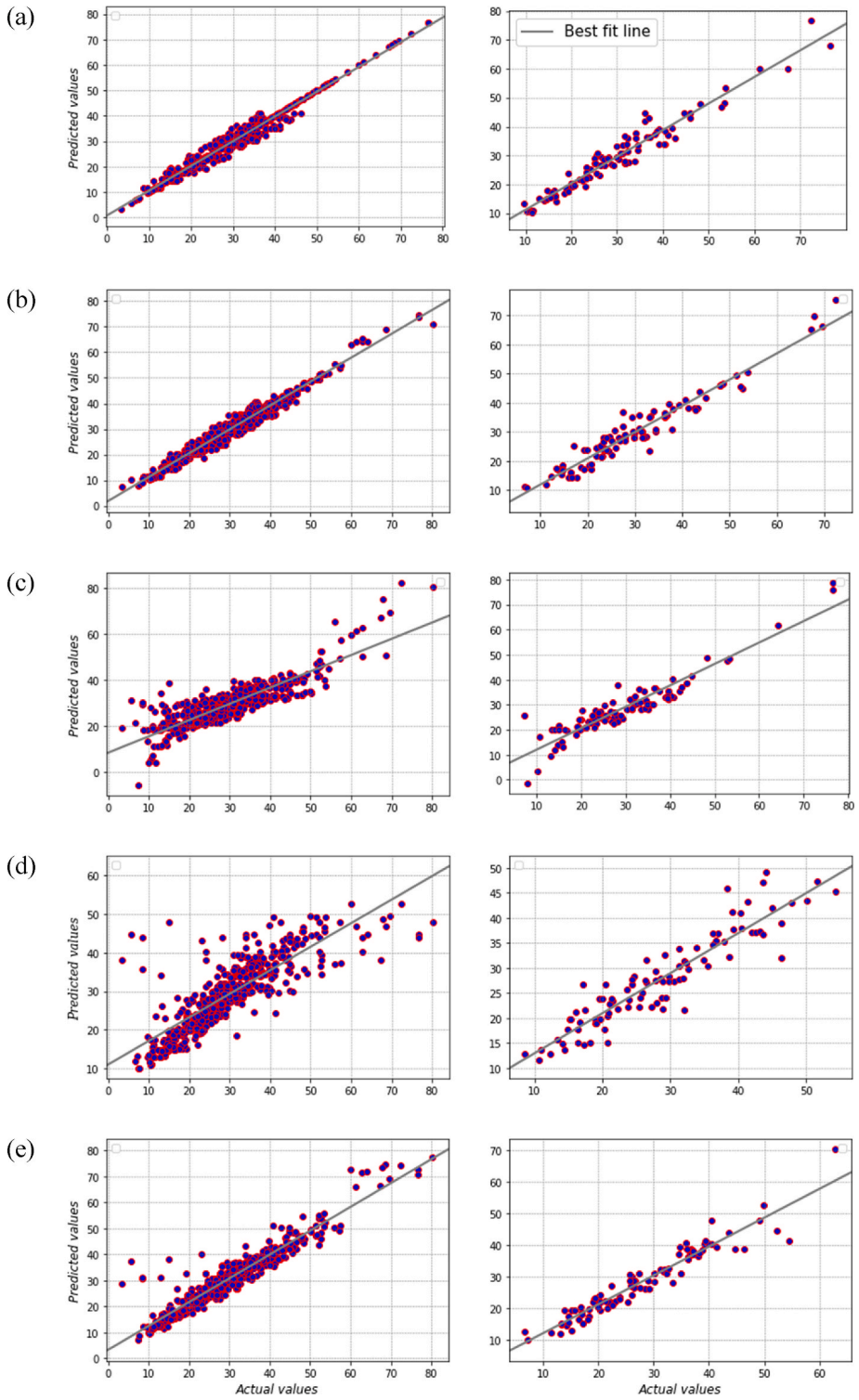

Fig. 8. Correlation between the predicted and actual values for (a) DT, (b) RF, (c) SVM, (d) KNN and (e) ANN.

incorporating GGBFS in different testing ages of 3 days, 7 days and 28 days as given in Equations 6a-c, respectively:

$$f'_{c,GGBFS} = \left[-0.465\left(\frac{G}{C}\right) + 0.968 \right] \times f'_c \quad \left(R^2 = 0.97\right) \tag{6a}$$

$$f'_{c,GGBFS} = \left[-0.532\left(\frac{G}{C}\right) + 1.010 \right] \times f'_c \quad \left(R^2 = 0.88\right) \tag{6b}$$

$$f'_{c,GGBFS} = \left[-0.320\left(\frac{G}{C}\right) + 1.039 \right] \times f'_c \quad \left(R^2 = 0.86\right) \tag{6c}$$

where f'_c is the compressive strength of normal concrete with a specific mixture, $f'_{c,GGBFS}$ is the compressive strength of the concrete containing GGBFS and the same mixture as the normal concrete, and (G/C) is the ratio of GGBFS to cement. AS could be observed in Equations 6a-c, the compressive strength of concrete with GGBFS is a function of the cement

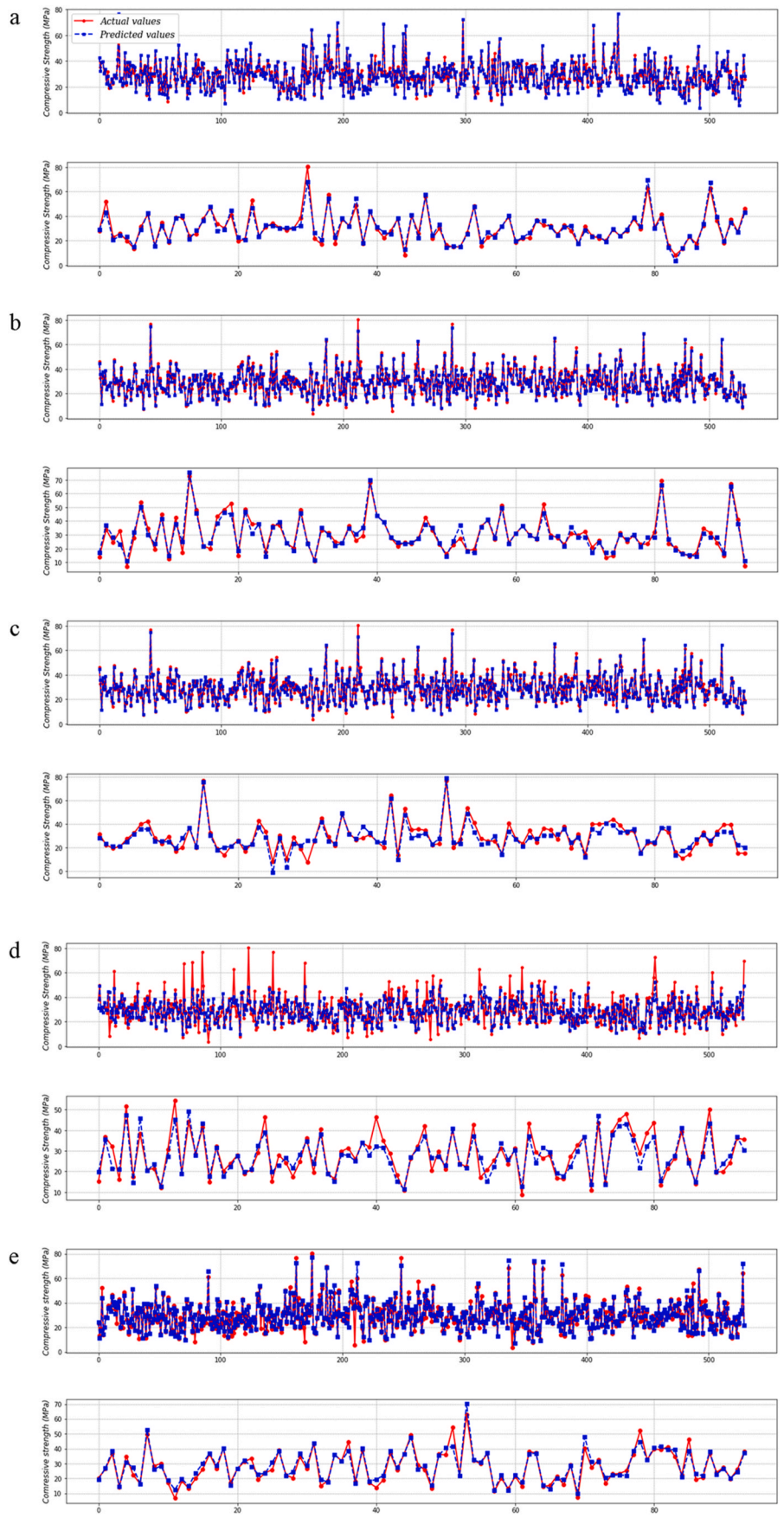

Fig. 9. Comparing the actual values with the predicted values for (a) DT, (b) RF, (c) SVM, (d) KNN, and (e) ANN.

Table 4
Performance metrics of the proposed prediction models.

	Equation	DT	RF	SVM	KNN	ANN
R^2	$\frac{\sum_i\left(\hat{y}_i-\frac{1}{n}\sum_1^n y_i\right)^2}{\sum_i\left(y_i-\frac{1}{n}\sum_1^n y_i\right)^2}$	0.94	0.94	0.87	0.85	0.92
R	$\sqrt{\frac{\sum_i\left(\hat{y}_i-\frac{1}{n}\sum_1^n y_i\right)^2}{\sum_i\left(y_i-\frac{1}{n}\sum_1^n y_i\right)^2}}$	0.97	0.97	0.93	0.92	0.96
RMSE (MPa)	$\sqrt{\frac{1}{n}\sum_1^n(\hat{y}_i-y_i)^2}$	3.18	3.32	4.5	4.08	3.10
MSE	$\frac{1}{n}\sum_1^n(\hat{y}_i-y_i)^2$	10.11	11.02	20.25	16.64	9.61
MAE (MPa)	$\frac{1}{n}\sum_1^n\lvert\hat{y}_i-y_i\rvert$	2.36	2.60	3.52	3.17	2.36
MAPE	$\frac{1}{n}\sum_1^n\left\lvert\frac{\hat{y}_i-y_i}{y_i}\right\rvert$	8.00	10.49	16.91	46.11	9.27

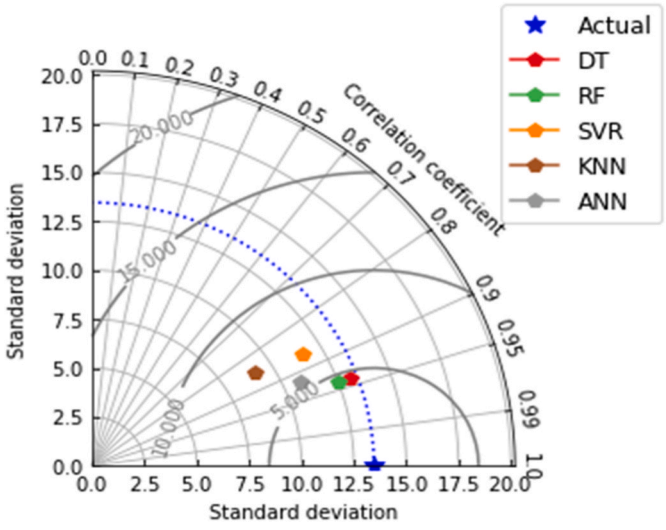

Fig. 10. Comparison of the models by Taylor diagram.

replaced by GGBFS and the compressive strength of normal concrete. Otherwise noted, an equation independent of normal concrete compressive strength could not be given because the strength of GGBFS concrete is highly dependent on the concrete mixture (e.g., water, fine and coarse aggregate, etc.). For example, the 3-day compressive strength of concrete with a specific mixture in which GGBFS replaces cement by 20% would be $0.875f'_c$, where f'_c is the compressive strength of the concrete without GGBFS and the same mixture.

Regarding GGBFS grade, the predicted values fluctuated for different grades considered in this study. Similar conclusions have also been made in previous research (Xu et al., 2014). Using the predicted values illustrated in Fig. 12, a prediction equation with $R^2 = 1.00$ is suggested for obtaining f'_c when GGBFS grade (GG) changes:

$$f'_{c,GGBFSi} = \left[1.156\times10^{-5}GG^2 - 0.0258GG + 2.326\right]\times f'_{c,GGBFS80} \quad \left(R^2 = 1.00\right) \tag{7}$$

where $f'_{c,GGBFSi}$ is the compressive strength of concrete containing GGBFS grade i, GG is the GGBFS grade and $f'_{c,GGBFS80}$ is the compressive strength of concrete incorporating GGBFS grade 80. By implementing Equations 6a-c into equation (7), the compressive strength of a concrete mixture with a specified f'_c in which cement is replaced with GGBFS by G/C ratio and grade GG could be determined by equations 8a, b and c, respectively after 3, 7 and 28 days:

$$f'_{c,GGBFSi,3-day} = \left[1.156\times10^{-5}GG^2 - 0.0258GG + 2.326\right] \times\left[-0.465\left(\frac{G}{C}\right)+0.986\right]\times f'_c \tag{8a}$$

$$f'_{c,GGBFSi,7-day} = \left[1.156\times10^{-5}GG^2 - 0.0258GG + 2.326\right] \times\left[-0.532\left(\frac{G}{C}\right)+1.010\right]\times f'_c \tag{8b}$$

$$f'_{c,GGBFSi,28-day} = \left[1.156\times10^{-5}GG^2 - 0.0258GG + 2.326\right] \times\left[-0.320\left(\frac{G}{C}\right)+1.039\right]\times f'_c \tag{8c}$$

8. Conclusions

The main objective of this study was to compare the accuracy of ML-based techniques for predicting the compressive strength of concrete containing GGBFS. To this end, a database including 625 results of experimental tests was collected from peer-reviewed international

Table 5
Variation of concrete compressive strength by changing GGBFS value and grade.

	OPC	G/C	GGBFS grade	W	CA	FA	Testing Age	f'c (MPa)	$(f'_{c,i}-f'_{c,1})/f'_{c,1}$
1	450	0.00	80	225	961.70	668.30	3	20.64	0.00
2	360	0.20	80	225	961.70	668.30	3	18.07	−12.44
3	270	0.40	80	225	961.70	668.30	3	17.26	−16.38
4	180	0.60	80	225	961.70	668.30	3	13.47	−34.72
5	90	0.80	80	225	961.70	668.30	3	12.79	−38.05
6	0	1.00	80	225	961.70	668.30	3	11.14	−46.04
7	450	0.00	80	225	961.70	668.30	7	29.28	0.00
8	360	0.20	80	225	961.70	668.30	7	27.08	−7.51
9	270	0.40	80	225	961.70	668.30	7	25.53	−12.82
10	180	0.60	80	225	961.70	668.30	7	16.65	−43.12
11	90	0.80	80	225	961.70	668.30	7	15.90	−45.70
12	0	1.00	80	225	961.70	668.30	7	15.96	−45.51
13	450	0.00	80	225	961.70	668.30	28	38.96	0.00
14	360	0.20	80	225	961.70	668.30	28	39.05	0.24
15	270	0.40	80	225	961.70	668.30	28	39.30	0.89
16	180	0.60	80	225	961.70	668.30	28	31.87	−18.20
17	90	0.80	80	225	961.70	668.30	28	28.88	−25.88
18	0	1.00	80	225	961.70	668.30	28	28.68	−26.39
19	450	0.25	80	225	961.70	668.30	28	40.32	0.00
21	450	0.25	100	225	961.70	668.30	28	36.28	−10.02
23	450	0.25	120	225	961.70	668.30	28	35.97	−10.79

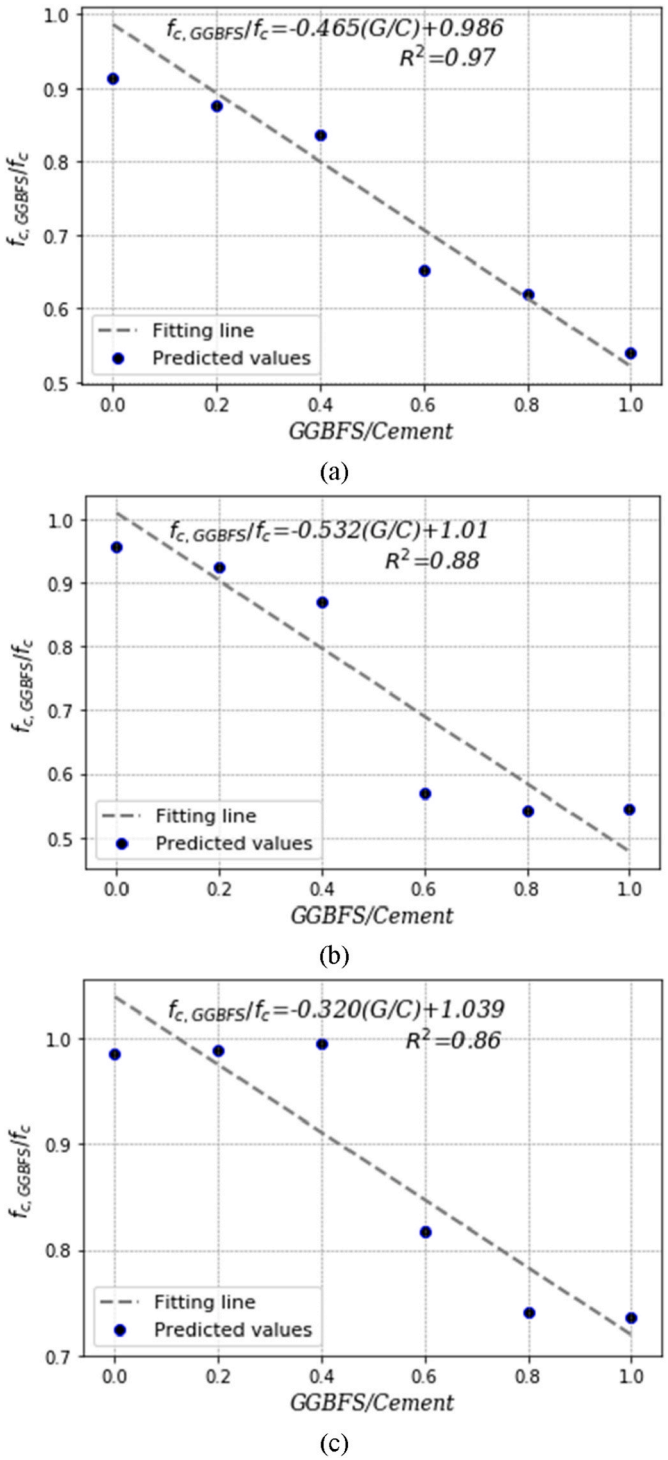

Fig. 11. Variation of $f'_{c,GGBFS}/f'_c$ ratio by changing GGBFS to Cement ratio after (a) 3 days, (7) days and (c) 28 days.

publications. The collected database was divided into two sub-databases: training (85%) and testing (15%). The input variables were ordinary Portland cement (OPC, kg/m^3), GGBFS to cement ratio (G/C), GGBFS grade, water (W, kg/m^3), coarse aggregate (CA, kg/m^3), fine aggregate (FA, kg/m^3) and testing age (days), and the output was concrete compressive strength. Decision Tree, Random Forest, Support Vector Machine, K-nearest Neighbors and Artificial Neural Networks models were developed. The predicted values by each model were compared to the actual values using performance metrics and the Taylor diagram. A sensitivity analysis was also conducted to determine the

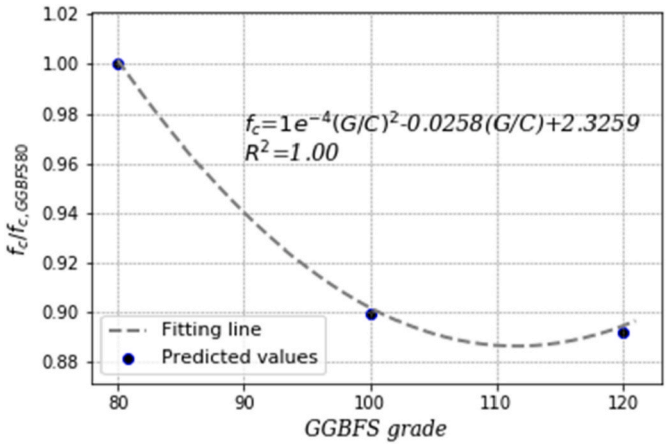

Fig. 12. Variation of f'_c by changing GGBFS grade.

effect of GGBFS value and grade on concrete compressive strength. Based on the results, it could be concluded that:

- All the proposed models were able to learn the relationship between the input variables and the output properly. Furthermore, the high accuracy of the predicted values confirms the reliability of the ML-based prediction models. Otherwise noted, ML-based models could be considered as inexpensive and quick methods for determining the compressive strength of concrete incorporating GGBFS instead of time-consuming and costly experimental tests.
- Among all the proposed models, the DT model exhibited the highest accuracy with $R^2 = 0.96$ and the KNN model had the lowest accuracy with $R^2 = 0.82$. However, the reliability of the all-proposed models could be considered acceptable with an R^2-score higher than 0.82.
- The performance of other ML-based methods (e.g., M5P trees) and regression-based techniques (e.g., linear, nonlinear, and ridge regression) is not considered in this study; therefore, they could be evaluated in further studies.
- The parametric study results clarified that by increasing the GGBFS to cement value in a concrete mixture, generally, f'_c reduces in any testing ages (3-, 7- and 28-day testing ages in this study). More specifically, replacing cement with GGBFS up to 100% decreased concrete compressive strength up to 45.51%. Furthermore, changing the GGBFS grade led to a fluctuation in f'_c. However, the mixture containing GGBFS grade 80 exhibited the highest compressive strength.

Declaration of competing interest

The authors declare that they have no conflict of interest.

Data availability

Data will be made available on request.

Acknowledgment

This work is a part of the TRANSFORM project. TRANSFORM has received funding from the Directorate for Higher Education and Competence (HK-dir), in Norway, under grant agreement UTF- 2020/10107.

References

abhekar, K.N., P, B., Pawade, Prashant, 2017. An experimental investigation of concrete on partial replacement of GGBS with cement. Int. J. Civ. Eng. Technol. 8, 418–427.
Abiodun, O.I., et al., 2018. State-of-the-art in artificial neural network applications: a survey. Heliyon 4 (11), e00938.

Ahmadi, M., et al., 2020. New empirical approach for determining nominal shear capacity of steel fiber reinforced concrete beams. Construct. Build. Mater. 234, 117293.
Amin, M.N., et al., 2017. Influence of mechanically activated electric arc furnace slag on compressive strength of mortars incorporating curing moisture and temperature effects. Sustainability 9 (8), 1178.
Amin, M.N., et al., 2021. Comparison of machine learning approaches with traditional methods for predicting the compressive strength of rice husk ash concrete. Crystals 11 (7), 779.
Anand, V., Kumar, A.P., Bhat, A.V., 2017. An experimental investigation on the performance of high volume ground granulated blast furnace slag concrete. Int. J. Civ. Eng. Technol. 8 (2).
Arivalagan, S., 2014. Sustainable studies on concrete with GGBS as a replacement material in cement. Jordan J. civil Eng. 8 (3), 263–270.
Band, S.S., et al., 2021. Groundwater level prediction in arid areas using wavelet analysis and Gaussian process regression. Engineering Applications of Computational Fluid Mechanics 15 (1), 1147–1158.
Becknell, N.K., Hale, W.M., 2005. Ternary concrete mixtures containing ground granulated blast furnace slag and fly ash. In: Cement Combinations for Durable Concrete: Proceedings of the International Conference Held at the University of Dundee. Thomas Telford Publishing, Scotland, UK on 5–7 July 2005.
Bellini, T., 2019. IFRS 9 and CECL Credit Risk Modelling and Validation: A Practical Guide with Examples Worked in R and SAS. Academic Press.
Benhelal, E., et al., 2013. Global strategies and potentials to curb CO2 emissions in cement industry. J. Clean. Prod. 51, 142–161.
Berman, J.J., 2016. Data Simplification: Taming Information with Open Source Tools. Morgan Kaufmann.
Bhattacharya, G., Ghosh, K., Chowdhury, A.S., 2017. Granger causality driven AHP for feature weighted kNN. Pattern Recogn. 66, 425–436.
Bhojaraju, C., et al., 2021. Fresh and hardened properties of GGBS-contained cementitious composites using graphene and graphene oxide. Construct. Build. Mater. 300, 123902.
Bilim, C., et al., 2009. Predicting the compressive strength of ground granulated blast furnace slag concrete using artificial neural network. Adv. Eng. Software 40 (5), 334–340.
Boğa, A.R., Öztürk, M., Topcu, I.B., 2013. Using ANN and ANFIS to predict the mechanical and chloride permeability properties of concrete containing GGBFS and CNI. Compos. B Eng. 45 (1), 688–696.
Breiman, L., 2001. Random forests. Mach. Learn. 45 (1), 5–32.
Bypour, M., Kioumarsi, M., Yekrangnia, M., 2021. Shear capacity prediction of stiffened steel plate shear walls (SSPSW) with openings using response surface method. Eng. Struct. 226, 111340.
Chaabene, W.B., Flah, M., Nehdi, M.L., 2020. Machine learning prediction of mechanical properties of concrete: critical review. Construct. Build. Mater. 260, 119889.
Chand, G., 2021. Microstructural study of sustainable cements produced from industrial by-products, natural minerals and agricultural wastes: a critical review on engineering properties. Cleaner Eng. Technol. 4, 100224.
Chand, G., et al., 2021. Microstructural and engineering properties investigation of sustainable hybrid concrete produced from industrial wastes. Cleaner Eng. Technol. 2, 100052.
Cheng, A., et al., 2005. Influence of GGBS on durability and corrosion behavior of reinforced concrete. Mater. Chem. Phys. 93 (2–3), 404–411.
Chidiac, S., Panesar, D., 2008. Evolution of mechanical properties of concrete containing ground granulated blast furnace slag and effects on the scaling resistance test at 28 days. Cement Concr. Compos. 30 (2), 63–71.
Cortes, C., Vapnik, V., 1995. Support-vector networks. Mach. Learn. 20 (3), 273–297.
Cover, T., Hart, P., 1967. Nearest neighbor pattern classification. IEEE Trans. Inf. Theor. 13 (1), 21–27.
Cramer, S., Sippel, C., 2005. Effects of Ground Granulated Blast Furnace Slag in Portland Cement Concrete. Wisconsin Highway Research Program.
Cwirzen, A., 2020. Properties of SCC with industrial by-products as aggregates. In: Self-Compacting Concrete: Materials, Properties and Applications. Elsevier, pp. 249–281.
Dabhekar, K., Nagarnaik, P., Pawade, P., 2017. Relationship between compressive strength and UPV for concrete with partial replacement of GGBFS. Int. J. Civ. Eng. Technol. 8 (5), 582–592.
Dabiri, H., et al., 2018. The influence of replacing sand with waste glass particle on the physical and mechanical parameters of concrete. Civil Eng. J. 4 (7), 1646–1652.
Dabiri, H., Kheyroddin, A., Faramarzi, A., 2022a. Predicting tensile strength of spliced and non-spliced steel bars using machine learning-and regression-based methods. Construct. Build. Mater. 325, 126835.
Dabiri, H., et al., 2022b. A machine learning-based analysis for predicting fragility curve parameters of buildings. J. Build. Eng. 62, 105367.
Deboucha, W., et al., 2015. Effect of incorporating blast furnace slag and natural pozzolana on compressive strength and capillary water absorption of concrete. Procedia Eng. 108, 254–261.
Dukart, J., 2015. Basic concepts of image classification algorithms applied to study neurodegenerative diseases. In: Brain Mapping: an Encyclopedic Reference. Elsevier, pp. 641–646.
Duxson, P., 2009. Geopolymer precursor design. In: Geopolymers. Elsevier, pp. 37–49.
El-Hassan, H., Kianmehr, P., 2018. Pervious concrete pavement incorporating GGBS to alleviate pavement runoff and improve urban sustainability. Road Mater. Pavement Des. 19 (1), 167–181.
Farahzadi, L., Kioumarsi, M., 2022a. Application of machine learning initiatives and intelligent perspectives for CO_2 emissions reduction in construction. J. Clean. Prod., 135504
Farahzadi, L., Kioumarsi, M., 2022b. Intelligent initiative to reduce CO2 emissions in construction. In: 8th European Congress on Computational Methods in Applied Sciences and Engineering (ECCOMAS Congress 2022), 1476.
Fawagreh, K., Gaber, M.M., Elyan, E., 2014. Random forests: from early developments to recent advancements. Systems Science & Control Engineering: An Open Access J. 2 (1), 602–609.
Fix, E., Hodges, J.L., 1989. Discriminatory analysis. Nonparametric discrimination: consistency properties. Int. Statist. Rev./Revue Internationale de Statistique 57 (3), 238–247.
Golafshani, E.M., et al., 2012. Prediction of bond strength of spliced steel bars in concrete using artificial neural network and fuzzy logic. Construct. Build. Mater. 36, 411–418.
Gowri, T.V., Sravana, P., Rao, P.S., 2016. On the relationship between compressive strength and water binder ratio of high volumes of slag concrete. Int. J. Appl. Eng. Res. 11 (2), 1436–1442.
Kandiri, A., Golafshani, E.M., Behnood, A., 2020. Estimation of the compressive strength of concretes containing ground granulated blast furnace slag using hybridized multi-objective ANN and salp swarm algorithm. Construct. Build. Mater. 248, 118676.
Kandiri, A., Sartipi, F., Kioumarsi, M., 2021. Predicting compressive strength of concrete containing recycled aggregate using modified ann with different optimization algorithms. Appl. Sci. 11 (2), 485.
Kioumarsi, M., et al., 2020. Effect of shrinkage reducing admixture on drying shrinkage of concrete with different w/c ratios. Materials 13 (24), 5721.
Klambauer, G., et al., 2017. Self-normalizing neural networks. In: Proceedings of the 31st International Conference on Neural Information Processing Systems.
Kotu, V., Deshpande, B., 2018. Data Science: Concepts and Practice. Morgan Kaufmann.
Kumar, R., et al., 2017. Relation among mechanical properties of ground granulated blast furnace slag concrete. Int. J. Civ. Eng. Technol. 8 (3).
LaBarca, I.K., Foley, R.D., Cramer, S.M., 2007. Effects of Ground Granulated Blast Furnace Slag in Portland Cement Concrete: Expanded Study. Wisconsin Highway Research Program.
Lee, K., et al., 2006. Autogenous shrinkage of concrete containing granulated blast-furnace slag. Cement Concr. Res. 36 (7), 1279–1285.
Li, G., Zhao, X., 2003. Properties of concrete incorporating fly ash and ground granulated blast-furnace slag. Cement Concr. Compos. 25 (3), 293–299.
Liu, S., et al., 2015. Computational and Statistical Methods for Analysing Big Data with Applications. Academic Press.
Mai, H.-V.T., et al., 2021a. Investigation of ANN model containing one hidden layer for predicting compressive strength of concrete with blast-furnace slag and fly ash. Adv. Mater. Sci. Eng. 2021.
Mai, H.-V.T., et al., 2021b. Prediction compressive strength of concrete containing GGBFS using random forest model. Adv. Civ. Eng. 2021.
Mishra, M., 2021. Machine learning techniques for structural health monitoring of heritage buildings: a state-of-the-art review and case studies. J. Cult. Herit. 47, 227–245.
Mohana, M.H., 2020. The determination of ground granulated concrete compressive strength based machine learning models. Period. Eng. Nat. Sci. 8 (2), 1011–1023.
Moradi, M.J., et al., 2020. Prediction of the load-bearing behavior of SPSW with rectangular opening by RBF network. Appl. Sci. 10 (3), 1185.
Nagendra, V., et al., 2016. GGBS and nano silica (NS) effect on concrete. Int. J. Civ. Eng. Technol. 7 (5), 477–484.
Naik, B.K., et al., 2021. Performance assessment of waste heat/solar driven membrane-based simultaneous desalination and liquid desiccant regeneration system using a thermal model and KNN machine learning tool. Desalination 505, 114980.
Nettleton, D., 2014. Commercial Data Mining: Processing, Analysis and Modeling for Predictive Analytics Projects. Elsevier.
Nisbet, R., Elder, J., Miner, G.D., 2009. Handbook of Statistical Analysis and Data Mining Applications. Academic press.
Oner, A., Akyuz, S., 2007. An experimental study on optimum usage of GGBS for the compressive strength of concrete. Cement Concr. Compos. 29 (6), 505–514.
Ozcan, G., Kocak, Y., Gulbandilar, E., 2017. Estimation of compressive strength of BFS and WTRP blended cement mortars with machine learning models. Comput. Concr. 19 (3), 275–282.
Samad, S., Shah, A., Limbachiya, M.C., 2017. Strength development characteristics of concrete produced with blended cement using ground granulated blast furnace slag (GGBS) under various curing conditions. Sādhanā 42 (7), 1203–1213.
Sarıdemir, M., et al., 2009. Prediction of long-term effects of GGBFS on compressive strength of concrete by artificial neural networks and fuzzy logic. Construct. Build. Mater. 23 (3), 1279–1286.
Satapathy, S.K., et al., 2019. EEG Brain Signal Classification for Epileptic Seizure Disorder Detection. Academic Press.
Sengul, O., Tasdemir, M.A., 2009. Compressive strength and rapid chloride permeability of concretes with ground fly ash and slag. J. Mater. Civ. Eng. 21 (9), 494–501.
Shahmansouri, A.A., Bengar, H.A., Ghanbari, S., 2020. Compressive strength prediction of eco-efficient GGBS-based geopolymer concrete using GEP method. J. Build. Eng. 31, 101326.
Shobha, G., Rangaswamy, S., 2018. Machine learning. In: Handbook of Statistics. Elsevier, pp. 197–228.
Shokrzade, A., et al., 2021. A novel extreme learning machine based kNN classification method for dealing with big data. Expert Syst. Appl., 115293
Sridevi, G., et al., 2016. Studies on strength properties of concrete with partial replacement of cement by GGBS. Int. J. Sci. Eng. Res. 7 (11), 946–949.
Taylor, K.E., 2001. Summarizing multiple aspects of model performance in a single diagram. J. Geophys. Res. Atmos. 106 (D7), 7183–7192.
Vapnik, V., 1999. The Nature of Statistical Learning Theory. Springer science & business media.

Wang, L., Chen, M.L., Tsang, D.C., 2020. Green remediation by using low-carbon cement-based stabilization/solidification approaches. In: Sustainable Remediation of Contaminated Soil and Groundwater. Elsevier, pp. 93–118.

Williams, B., et al., 2020. Data-Driven model development for cardiomyocyte production experimental failure prediction. In: Computer Aided Chemical Engineering. Elsevier, pp. 1639–1644.

Xu, H., et al., 2014. Effect of blast furnace slag grades on fly ash based geopolymer waste forms. Fuel 133, 332–340.